Adaptive Human Pilot Model for Uncertain Systems

S. S. Tohidi[1] and Y. Yildiz[1]

***Abstract*— Inspired by humans' ability to adapt to changing environments, this paper proposes an adaptive human model that mimics the crossover model despite input bandwidth deviations and plant uncertainties. The proposed human model structure is based on the model reference adaptive control, and the adaptive laws are obtained using the Lyapunov-Krasovskii stability criteria applied to the overall closed loop system including the human pilot, the controller and the plant. The proposed model can be employed for human-in-the-loop stability analysis with different controllers and plant types. A numerical example is used to demonstrate the effectiveness of the presented method.**

I. INTRODUCTION

Unique abilities of humans such as adaptive behavior in dynamic environments, and social interaction and moral judgment capabilities, make humans essential elements of in most control loops, operating in close collaboration with autonomy. On the other hand, autonomy provides higher computational performance and multi-tasking capabilities without any fatigue, stress, or boredom [1], [2].

Apart from their individual strengths, humans and autonomy have their own weaknesses. Compared to automatic control, the probability of human error causing system failure is higher. Moreover, humans may have anxiety, fear and unconsciousness during operations. In the tasks that require increased attention and focus, humans may tend to provide high gain control inputs which can cause undesired oscillations. One example of this phenomenon, for example, is the occurance of pilot induced oscillations (PIO), where undesired and sustained oscillations are observed due to an abnormal coupling between the aircraft and the pilot [3], [4], [5], [6]. Similarly, there exists cases, where the autonomy fails due to an uncertainty, fault or cyber-attack [7]. Thus, it may be more preferable to design systems where humans and automation work in harmony, complementing each other, resulting in a structure that benefits from the advantages of both.

A mathematically rigorous investigation of human in the loop dynamics help develop safe control mechanisms, and provide a better realization and understanding of human control actions and limitations [8], [9], [10]. To achieve this purpose, reliable human mathematical models are required. One of the first human models in aeronautics is proposed in [11], called the Neal-Smith model, as a transfer function which can be used in closed loop stability analysis. In [12], [13] it is stated that every control intention has to be translated to a body movement by the neuromuscular system and a transfer function model is proposed illustrating this observation. Crossover model, another human pilot model defined in [14], is motivated from the empirical observation that human pilots adapt their responses in such a way that the overall open loop system dynamics resembles that of a well-designed feedback system. Several approaches are developed to identify the parameters of the two fundamental models, Neal-Smith and neuromuscular models in [15], a two-step method using wavelets and a windowed maximum likelihood estimation method are exploited for the estimation of time-varying pilot model parameters. In [16], the Linear Parameter Varying model identification framework is incorporated to estimate time-varying human state space representation matrices. Subsystem identification is used in [17] to model the control strategies of the human in the loop. In comparison with the estimation based methods the proposed method does not require system identification or estimation methods.

There also exist pilot models in the literature that mimics the adaptation ability of humans. In [18] and [19], the adaptive behavior of human in the loop is formulated and adaptive rules are provided based on an expert experiences about human adaptive behavior in the control loop. It is illustrated that the proposed adaptive human model follows the crossover model. A survey on various human models can be found in [20] and [21].

In this paper, we propose, proposes an adaptive human pilot model that modifies its behavior based on deviations in the forcing function (reference input) bandwidth and plant uncertainties. In addition, the closed loop system with the proposed human model is shown to follow the output of the crossover model without expert experience requirements. The adaptive laws are obtained based on the Lyapunov-Krasovskii stability criteria.

This paper is organized as follow. Section II presents the crossover law briefly, and states the dynamics of plant, human neuromuscular and reference model. Obtaining reference model parameters are discussed in Section III. Section IV presents the human adaptive control strategy and the stability analysis. A numerical example is used in Section V to illustrate the effectiveness of the proposed methodology in the simulation environment. Finally, Section VI concludes the paper.

II. PROBLEM STATEMENT

According to McRuer's crossover model [14], human pilots in the control loop behave in a way that results in

*This work was not supported by any organization

[1]S. S. Tohidi and Y. Yildiz are with Faculty of Mechanical Engineering, Bilkent University, Cankaya, Ankara 06800, Turkey {shahabaldin, yyildiz}@bilkent.edu.tr

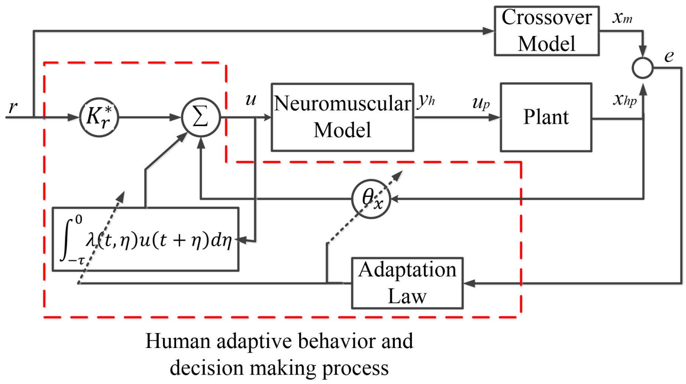

Fig. 1: The block diagram of the human adaptive behavior and decision making in closed loop system.

an open loop transfer function

$$Y_{OL}(s) = Y_h(s)Y_p(s) = \frac{\omega_c e^{-\tau s}}{s}, \tag{1}$$

near the crossover frequency (ω_c), where Y_h is the transfer function of the human pilot and Y_p is the transfer function of the plant. Also, τ is the effective time delay, including transport delays and high frequency neuromuscular lags, and ω_c is the open loop gain which can be considered as pilot gain.

Consider the following plant dynamics

$$\dot{x}_p(t) = A_p x_p(t) + B_p u_p(t), \tag{2}$$

where $x_p \in R^{n_p}$ is the plant state vector, $u_p \in R^{m_p}$ is the plant input vector, $A_p \in R^{n_p \times n_p}$ is an unknown plant state matrix, $B_p \in R^{n_p \times m_p}$ is an unknown plant control matrix.

The approximate human neuromuscular model [22] is represented in state space form which is given as

$$\begin{aligned} \dot{x}_h(t) &= A_h x_h(t) + B_h u(t-\tau) \\ y_h(t) &= C_h x_h(t) + D_h u(t-\tau), \end{aligned} \tag{3}$$

where $A_h \in R^{n_h \times n_h}$ is the known neuromuscular state matrix, $B_h \in R^{n_h \times m_h}$ is the known neuromuscular control matrix, $C_h \in R^{m_p \times n_h}$ is the known neuromuscular output matrix, and $D_h \in R^{m_p \times m_h}$. Also $x_h \in R^{n_h}$ is the neuromuscular state vector, $u \in R^{m_h}$ is the neuromuscular input vector, $y_h \in R^{m_p}$ is the neuromuscular output vector, and $\tau \in R^{+}$ is a known, constant delay. In this structure, the output of the human neuromuscular model, y_h, is used as the plant input u_p in (2), that is $y_h = u_p$(see figure 1).

By combining the human pilot and plant states, we obtain the open loop human-plant dynamics as

$$\begin{aligned} \underbrace{\begin{bmatrix} \dot{x}_h(t) \\ \dot{x}_p(t) \end{bmatrix}}_{\dot{x}_{hp}(t)} &= \underbrace{\begin{bmatrix} A_h & 0_{n_h \times n_p} \\ B_p C_h & A_p \end{bmatrix}}_{A_{hp}} \underbrace{\begin{bmatrix} x_h(t) \\ x_p(t) \end{bmatrix}}_{x_{hp(t)}} \\ &+ \underbrace{\begin{bmatrix} B_h \\ B_p D_h \end{bmatrix}}_{B_{hp}} u(t-\tau), \end{aligned} \tag{4}$$

TABLE I

Plant transfer function	Crossover frequency of the open loop transfer function
K	$\omega_c = 0.067\omega_i^2 + 0.099\omega_i + 4.8$
K/s	$\omega_c = 0.14\omega_i + 4.3$
K/s^2	$\omega_c = -0.0031\omega_i^4 - 0.072\omega_i^3 + 0.29\omega_i^2$ $-0.13\omega_i + 3$

which can be written in the following compact form

$$\dot{x}_{hp}(t) = A_{hp} x_{hp}(t) + B_{hp} u(t-\tau), \tag{5}$$

where $x_{hp} = [x_h^T \ \ x_p^T]^T \in R^{(n_p+n_h)}$, $A_{hp} \in R^{(n_p+n_h)\times(n_p+n_h)}$, $B_{hp} \in R^{(n_p+n_h)\times m_h}$.

The goal is to obtain the input $u(t)$ in (3), which is the control decision of the pilot, such that the closed loop system consisting of the adaptive human pilot model and the plant follow the output of a unity feedback reference model with an open loop crossover transfer function

$$Y_{OL}(s) = \frac{\omega_c e^{-\tau s}}{s} \frac{(s+\alpha)^{n_p+n_h-1}}{(s+\alpha)^{n_p+n_h-1}}, \tag{6}$$

where α is a positive constant utilized to make the reference model order equal to that of the human-plant system. The reference model, whose open loop transfer function is given in (6), can be represented in state space form as

$$\dot{x}_m(t) = A_m x_m(t) + B_m r(t-\tau) \tag{7}$$

where $x_m \in R^{(n_h+n_p)}$ is the reference model state vector, $A_m \in R^{(n_h+n_p)\times(n_h+n_p)}$ is the state matrix, $B_m \in R^{(n_h+n_p)\times m_h}$ is the input matrix, and $r \in R^{m_h}$ is the reference input.

III. REFERENCE MODEL PARAMETERS

The crossover transfer function (6) contains the crossover frequency, ω_c, which is not known a priory. Experimental data, showing the reference input ($r(t)$) frequency bandwidth, ω_i, versus crossosover frequency ω_c, is provided in [14], for plant transfer functions K, K/s and K/s^2. We fit polynomials to these experimental results to obtain the crossover frequency of the open loop transfer function given a reference input frequency bandwidth. These polynomials are given in Table I. It is noted that when the reference input has multiple frequency components, the highest frequency is used to calculate the crossover frequency.

Remark 1. In this work, we use the polynomial relationships provided in Table I for zero, first and second order plant dynamics with nonzero poles and zeros. It is noted that further experimental work with humans are required to obtain more precise crossover vs reference input frequency relationships.

IV. HUMAN CONTROL COMMAND

The adaptive human decision command, $u(t)$, is determined as

$$u(t) = K_r K_x x_{hp}(t+\tau) + K_r r(t) \tag{8}$$

where $K_x \in R^{m_h \times (n_h+n_p)}$, and $K_r \in R^{m_h \times m_h}$. Using (8) and (5), the closed loop dynamics can be written as

$$\dot{x}_{hp}(t) = (A_{hp} + B_{hp}K_rK_x)x_{hp}(t) + B_{hp}K_r r(t-\tau). \tag{9}$$

Equation (8) describes a non-causal command which requires future values of the states. This problem can be eliminated by solving the differential equation (5) as a τ-seconds ahead predictor as

$$x_{hp}(t+\tau) = e^{A_{hp}\tau}x_{hp}(t) + \int_{-\tau}^{0} e^{-A_{hp}\eta}B_{hp}u(t+\eta)d\eta. \tag{10}$$

Assumption 1. There exist ideal parameters K_r^* and K_x^* satisfying the following matching conditions

$$\begin{aligned} A_{hp} + B_{hp}K_r^*K_x^* &= A_m \\ B_{hp}K_r^* &= B_m. \end{aligned} \tag{11}$$

By substituting (10) into (8), the control input can be written as

$$\begin{aligned} u(t) &= K_rK_xe^{A_{hp}\tau}x_{hp}(t) \\ &+ K_rK_x\int_{-\tau}^{0} e^{-A_{hp}\eta}B_{hp}u(t+\eta)d\eta + K_r r(t). \end{aligned} \tag{12}$$

By defining $\theta_x(t) = K_r(t)K_x(t)e^{A_{hp}\tau}$ and $\lambda(t,\eta) = K_r(t)K_x(t)e^{-A_{hp}\eta}B_{hp}$, we have (see figure 1)

$$u(t) = \theta_x(t)x_{hp}(t) + \int_{-\tau}^{0}\lambda(t,\eta)u(t+\eta)d\eta + K_r(t)r(t). \tag{13}$$

The ideal values of θ_x and λ can be obtained as

$$\begin{aligned} \theta_x^* &= K_r^*K_x^*e^{A_{hp}\tau} \\ \lambda^* &= K_r^*K_x^*e^{-A_{hp}\eta}B_{hp}. \end{aligned} \tag{14}$$

Since A_{hp} is unknown, θ_x and λ need to be estimated. The closed loop dynamics can be obtained using (5) and (13) as

$$\begin{aligned} \dot{x}_{hp}(t) &= A_{hp}x_{hp}(t) + B_{hp}\theta_x(t-\tau)x_{hp}(t-\tau) \\ &+ \int_{-\tau}^{0} B_{hp}\lambda(t-\tau,\eta)u(t+\eta-\tau)d\eta \\ &+ B_{hp}K_r r(t-\tau), \end{aligned} \tag{15}$$

Defining $\tilde{\theta}_x = \theta_x - \theta_x^*$, $\tilde{\lambda} = \lambda - \lambda^*$, and adding and subtracting $A_m x_{hp}(t)$ to (15), and using (11), (10) and (14), we have

$$\begin{aligned} \dot{x}_{hp}(t) &= A_m x_{hp}(t) + B_m r(t-\tau) + B_{hp}\tilde{\theta}_x(t-\tau)x_{hp}(t-\tau) \\ &+ B_{hp}\int_{-\tau}^{0}\tilde{\lambda}(t-\tau,\eta)u(t-\tau+\eta)d\eta. \end{aligned} \tag{16}$$

Defining the tracking error as $e(t) = x_{hp} - x_m$, and subtracting (7) from (5), it is obtained that

$$\begin{aligned} \dot{e}(t) &= \dot{x}_{hp} - \dot{x}_m \\ &= A_m e(t) + B_{hp}\tilde{\theta}_x(t-\tau)x_{hp}(t-\tau) \\ &+ B_{hp}\int_{-\tau}^{0}\tilde{\lambda}(t-\tau,\eta)u(t-\tau+\eta)d\eta. \end{aligned} \tag{17}$$

Theorem 1. Given the initial conditions $\tilde{\theta}_x(\xi)$, $\tilde{\lambda}(\xi,\eta)$ and $x_{hp}(\xi)$ for $\xi \in [-\tau, 0]$, and $u(\zeta)$ for $\zeta \in [-2\tau, 0]$, there exists a τ^* such that for all $\tau \in [0, \tau^*]$, the human-plant system (5), with the controller (13) and the following adaptive laws

$$\dot{\tilde{\theta}}_x^T(t) = -x_{hp}(t-\tau)e(t)^TPB_{hp}, \tag{18}$$

$$\dot{\tilde{\lambda}}^T(t,\eta) = -u(t+\eta-\tau)e(t)^TPB_{hp}, \tag{19}$$

follow the crossover model (7), while all the signals remain bounded.

Proof. Consider a Lyapunov-Krasovskii functional ([23]; [24])

$$\begin{aligned} V(t) &= e^TPe + tr(\tilde{\theta}_x^T(t)\tilde{\theta}_x(t)) \\ &+ \int_{-\tau}^{0}\int_{t+v}^{t} tr(\dot{\tilde{\theta}}_x^T(\xi)\dot{\tilde{\theta}}_x(\xi))d\xi dv \\ &+ \int_{-\tau}^{0} tr(\tilde{\lambda}^T(t,\eta)\tilde{\lambda}(t,\eta))d\eta \\ &+ \int_{-\tau}^{0}\int_{t+v}^{t}\int_{-\tau}^{0} tr(\dot{\tilde{\lambda}}^T(\xi,\eta)\dot{\tilde{\lambda}}(\xi,\eta))d\eta d\xi dv, \end{aligned} \tag{20}$$

where $\dot{\tilde{\lambda}} = \frac{\partial\tilde{\lambda}}{\partial t}$ and P is the positive definite symmetric matrix solution of the Lyapunov equation

$$A_m^TP + PA_m = -Q, \tag{21}$$

where Q is a symmetric positive definite matrix. The derivative of $V(t)$ can be calculated by using Leibniz's rule, that is $\frac{d}{dt}\int_{a(t)}^{b(t)} f(y)dy = f(b(t))\frac{db(t)}{dt} - f(a(t))\frac{da(t)}{dt}$, and the trace operator property $tr(X^TX) = ||X||_F^2$, as

$$\begin{aligned} \dot{V}(t) &= \dot{e}^T(t)^TPe(t) + e^T(t)P\dot{e}(t) + 2tr(\dot{\tilde{\theta}}_x^T(t)\tilde{\theta}_x(t)) \\ &\int_{-\tau}^{0} 2tr(\dot{\tilde{\lambda}}^T(t,\eta)\tilde{\lambda}(t,\eta))d\eta \\ &+ \tau||\dot{\tilde{\theta}}_x(t)||_F^2 - \int_{-\tau}^{0}||\dot{\tilde{\theta}}_x(t+v)||_F^2 dv \\ &+ \tau\int_{-\tau}^{0}||\dot{\tilde{\lambda}}(t,\eta)||_F^2 d\eta - \int_{-\tau}^{0}\int_{-\tau}^{0}||\dot{\tilde{\lambda}}(t+v,\eta)||_F^2 d\eta dv. \end{aligned} \tag{22}$$

Using (17) and (21), we have

$$\begin{aligned} \dot{V}(t) &= -e^T(t)Qe(t) + 2e^T(t)PB_{hp}\tilde{\theta}_x(t-\tau)x_{hp}(t-\tau) \\ &+ 2e^T(t)PB_{hp}\int_{-\tau}^{0}\tilde{\lambda}(t-\tau,\eta)u(t+\eta-\tau)d\eta \\ &+ 2tr(\dot{\tilde{\theta}}_x^T(t)\tilde{\theta}_x(t)) + \int_{-\tau}^{0} 2tr(\dot{\tilde{\lambda}}^T(t,\eta)\tilde{\lambda}(t,\eta))d\eta \\ &+ \tau||\dot{\tilde{\theta}}_x(t)||_F^2 - \int_{-\tau}^{0}||\dot{\tilde{\theta}}_x(t+v)||_F^2 dv \\ &+ \tau\int_{-\tau}^{0}||\dot{\tilde{\lambda}}(t,\eta)||_F^2 d\eta - \int_{-\tau}^{0}\int_{-\tau}^{0}||\dot{\tilde{\lambda}}(t+v,\eta)||_F^2 d\eta dv. \end{aligned} \tag{23}$$

Using $g(t)-g(t-\tau)=\int_{-\tau}^{0}\dot{g}(t+v)dv$, we have

$$
\begin{aligned}
\dot{V}(t) &= -e^T(t)Qe(t) \\
&+ 2tr\Big(x_{hp}(t-\tau)e^T(t)PB_{hp}\tilde{\theta}_x(t)+\dot{\tilde{\theta}}_x^T(t)\tilde{\theta}_x(t)\Big) \\
&+ \int_{-\tau}^{0} 2tr\Big(u(t+\eta-\tau)e^T(t)PB_{hp}\tilde{\lambda}(t,\eta) \\
&+ \dot{\tilde{\lambda}}^T(t,\eta)\tilde{\lambda}(t,\eta)\Big)d\eta \\
&- 2e^T(t)PB_{hp}(\int_{-\tau}^{0}\dot{\tilde{\theta}}_x(t+v)dv)x_{hp}(t-\tau) \\
&- 2e^T(t)PB_{hp}\Big(\int_{-\tau}^{0}(\int_{-\tau}^{0}\dot{\tilde{\lambda}}(t+v,\eta)dv)u(t+\eta-\tau)d\eta\Big) \\
&+ \tau||\dot{\tilde{\theta}}_x(t)||_F^2-\int_{-\tau}^{0}||\dot{\tilde{\theta}}_x(t+v)||_F^2dv \\
&+ \tau\int_{-\tau}^{0}||\dot{\tilde{\lambda}}(t,\eta)||_F^2d\eta-\int_{-\tau}^{0}\int_{-\tau}^{0}||\dot{\tilde{\lambda}}(t+v,\eta)||_F^2d\eta dv.
\end{aligned}
\tag{24}
$$

By substituting (18)-(19) into (24), we have

$$
\begin{aligned}
\dot{V}(t) &\le -e^T(t)Qe(t) \\
&- 2\int_{-\tau}^{0} tr(x_{hp}(t-\tau)e(t)^TPB_{hp}\dot{\tilde{\theta}}_x(t+v))dv \\
&- 2\int_{-\tau}^{0}\int_{-\tau}^{0} tr(u(t+\eta-\tau)e(t)^TPB_{hp}\dot{\tilde{\lambda}}(t+v,\eta))dvd\eta \\
&+ \tau||\dot{\tilde{\theta}}_x(t)||_F^2-\int_{-\tau}^{0}||\dot{\tilde{\theta}}_x(t+v)||_F^2dv \\
&+ \tau\int_{-\tau}^{0}||\dot{\tilde{\lambda}}(t,\eta)||_F^2d\eta-\int_{-\tau}^{0}\int_{-\tau}^{0}||\dot{\tilde{\lambda}}(t+v,\eta)||_F^2d\eta dv \\
&= -e^T(t)Qe(t)+2\int_{-\tau}^{0} tr(\dot{\tilde{\theta}}_x^T(t)\dot{\tilde{\theta}}_x(t+v))dv \\
&+ 2\int_{-\tau}^{0}\int_{-\tau}^{0} tr(\dot{\tilde{\lambda}}^T(t,\eta)\dot{\tilde{\lambda}}(t+v,\eta))dvd\eta \\
&+ \tau||\dot{\tilde{\theta}}_x(t)||_F^2-\int_{-\tau}^{0}||\dot{\tilde{\theta}}_x(t+v)||_F^2dv \\
&+ \tau\int_{-\tau}^{0}||\dot{\tilde{\lambda}}(t,\eta)||_F^2d\eta-\int_{-\tau}^{0}\int_{-\tau}^{0}||\dot{\tilde{\lambda}}(t+v,\eta)||_F^2d\eta dv \\
&= -e^T(t)Qe(t)+\int_{-\tau}^{0} tr\Big(2\dot{\tilde{\theta}}_x^T(t)\dot{\tilde{\theta}}_x(t+v) \\
&+ \dot{\tilde{\theta}}_x^T(t)\dot{\tilde{\theta}}_x(t)-\dot{\tilde{\theta}}_x^T(t+v)\dot{\tilde{\theta}}_x(t+v)\Big)dv \\
&+ \int_{-\tau}^{0}\int_{-\tau}^{0} tr\Big(2\dot{\tilde{\lambda}}^T(t,\eta)\dot{\tilde{\lambda}}(t+v,\eta) \\
&+ \dot{\tilde{\lambda}}^T(t,\eta)\dot{\tilde{\lambda}}(t,\eta)-\dot{\tilde{\lambda}}^T(t+v,\eta)\dot{\tilde{\lambda}}(t+v,\eta)\Big)d\eta dv.
\end{aligned}
\tag{25}
$$

By using the trace property $tr(A+B)=tr(A)+tr(B)$, and the algebraic inequality $a^2\ge 2ab-b^2$ for two scalars a and b, we have

$$
\begin{aligned}
\dot{V}(t) &\le -e^T(t)Qe(t)+\int_{-\tau}^{0}2tr\Big(\dot{\tilde{\theta}}_x^T(t)\dot{\tilde{\theta}}_x(t)\Big)dv \\
&+ \int_{-\tau}^{0}\int_{-\tau}^{0}2tr\Big(\dot{\tilde{\lambda}}^T(t,\eta)\dot{\tilde{\lambda}}(t,\eta)\Big)d\eta dv.
\end{aligned}
\tag{26}
$$

By substituting (18)-(19) into (25), and using the trace operator property $tr(AB)=tr(BA)$ for two matrices of proper dimension A and B, we have

$$
\begin{aligned}
\dot{V}(t) &\le -e^T(t)Qe(t) \\
&+ 2\tau tr\big(e(t)x_{hp}^T(t-\tau)x_{hp}(t-\tau)e(t)^TPB_{hp}B_{hp}^TP\big) \\
&+ 2\tau\int_{-\tau}^{0} tr\big(e(t)u^T(t-\tau+\eta)u(t+\eta-\tau)e(t)^T \\
&\times PB_{hp}B_{hp}^TP\big)d\eta.
\end{aligned}
\tag{27}
$$

By using the trace operator property $tr(AB)\le tr(A)tr(B)$ for two positive semidefinite matrices A and B (see [25]), we have

$$
\begin{aligned}
\dot{V}(t) &\le -e^T(t)Qe(t) \\
&+ 2\tau tr\big(e(t)x_{hp}^T(t-\tau)x_{hp}(t-\tau)e(t)^T\big)tr\big(PB_{hp}B_{hp}^TP\big) \\
&+ 2\tau\int_{-\tau}^{0} tr\big(e(t)u^T(t-\tau+\eta)u(t+\eta-\tau)e(t)^T\big) \\
&\times tr\big(PB_{hp}B_{hp}^TP\big)d\eta \\
&\le -\lambda_{min}(Q)||e(t)||^2+2\tau||x_{hp}(t-\tau)e(t)^T||_F^2||B_{hp}^TP||_F^2 \\
&+ 2\tau\int_{-\tau}^{0}||u(t+\eta-\tau)e(t)^T||_F^2||B_{hp}^TP||_F^2d\eta \\
&\le -\lambda_{min}(Q)||e(t)||^2+2\tau||x_{hp}(t-\tau)||^2||e(t)||^2||B_{hp}^TP||_F^2 \\
&+ 2\tau\int_{-\tau}^{0}||u(t+\eta-\tau)||^2||e(t)||^2||B_{hp}^TP||_F^2d\eta \\
&= ||B_{hp}^TP||_F^2||e(t)||^2\Big(-\frac{\lambda_{min}(Q)}{||B_{hp}^TP||_F^2} \\
&+ 2\tau\big(||x_{hp}(t-\tau)||^2+\int_{-\tau}^{0}||u(t+\eta-\tau)||^2d\eta\big)\Big)
\end{aligned}
\tag{28}
$$

By defining $q\equiv\frac{\lambda_{min}(Q)}{||B_{hp}^TP||_F^2}$, for the non-positiveness of $\dot{V}(t)$, we need to satisfy

$$
q-2\tau\big(||x_{hp}(t-\tau)||^2+\int_{-\tau}^{0}||u(t+\eta-\tau)||^2d\eta\big)\ge 0.
\tag{29}
$$

It may not be easy to check if (29) is satisfied since x_{hp} and u are dependent variables. The proof that shows (29) is satisfied for all time-delay values smaller than a certain value τ^*, and therefore x_{hp} and u are bounded for all $t>0$, is provided for a similar system in [23], using induction. Here, we provide a summary of the proof in the four steps:

Step 1: It is shown that (29) is satisfied for all $t\in[t_0,t_0+\tau]$. Using this result, an upper bound I_0, which is related to the $V(t_0)$, and a delay value τ_1 are found such that $||x_{hp}(\xi)||\le I_0$, and $||u(\xi)||\le g_1(I_0,\tau)$, $\forall\xi\in[t_0,t_0+\tau]$, $\forall\tau\in[0,\tau_1]$, where g_1 is a function of I_0, τ and known constants.

Step 2: A delay value τ_2 is found for which (29) is satisfied, which in turn leads to a non-increasing $\dot{V}(\xi)$ for $\forall\xi\in[t_0,t_0+2\tau]$, $\forall\tau\in[0,\bar{\tau}_2]$, $\bar{\tau}_2=\min(\tau_1,\tau_2)$. Using this result, it is shown that $||x_{hp}(\xi)||$ is bounded for $\forall\xi\in[t_0,t_0+2\tau]$, $\forall\tau\in[0,\bar{\tau}_2]$.

Step 3: It is shown that the maximum possible value of the control signal u in the interval $[t_0,t_0+\tau]$ is a function of only I_0, A_{hp}, B_{hp}, T and τ, where T is a value between t_0 and τ.

Step 4: It is shown that there exists a delay value τ_3 which leads to a non-increasing $\dot{V}(\xi)$ for $\forall \xi \in [t_0, t_0 + \tau]$, $\forall \tau \in [0, \tau^*]$, $\tau^* = \min(\bar{\tau}_2, \tau_3)$, and it is shown that $||x_{hp}(\xi)|| \leq I_0$ and $||u(\xi)|| \leq g_2$ for $\forall \xi \in [t_0, t_0 + \tau]$, $\forall \tau \in [0, \tau^*]$, where g_2 is a function of I_0 and other known constants.

The above four steps show that $||x_{hp}(\xi)|| \leq I_0$ and $||u(\xi)|| \leq g_2(I_0)$ for $\forall \xi \in [t_0, t_0 + k\tau]$, for $k = 1$ and $\tau \in (0, \tau^*]$. It is then shown that, if it is assumed that this is true for a given k, other than 1, then it must be true for $k+1$. This completes the proof using induction. For details, see [23].

Remark 2. In order to implement the control signal (13), the integral term is approximated as

$$\int_{-\tau}^{0} \lambda(t, \eta) u(t + \eta) d\eta \approx \lambda(t, -\tau) u(t - \tau) + \lambda(t, -\tau + d\eta) u(t - \tau + d\eta) + ... + \lambda(t, 0) u(t). \tag{30}$$

Remark 3. The crossover model is an integrator with crossover gain (ω_c) and time-delay (τ). The ω_c regression and τ increment reduce the phase margin which leads to the model instability. A comprehensive research about the variation of crossover model parameters is done in [12], [13] and [26]. Changing in ω_c with respect to the reference input bandwidth (ω_i) is considered in the proposed adaptive human model. In this model, the human effective time delay is assumed to be constant and known. A more accurate human adaptive model considering unknown human response delay will be analyzed in future work.

V. Simulation Results

A first order stable plant $Y_p(s) = \frac{4}{s+1}$ before $t = 25sec$ is considered. At $t = 25sec$, the plant transfer function will be changed to $Y_p(s) = \frac{2}{s+0.5}$. The neuromuscular dynamics of the system is given as $Y_h(s) = \frac{3}{s+2} e^{-0.3s}$, where the time delay $\tau = 0.3$ is the effective time delay, including human decision making delay and neuromuscular lags.

The reference signal (forcing function) is generated by summation of the sinusoid functions with different frequencies. The frequencies are 0.16, 0.4, 0.86, 1.33, $4.2 rad/sec$ and the amplitude of each is 0.2. Thus, the highest frequency component which shows the input bandwidth is $\omega_i = 4.2 rad/sec$. Using the table 1 for the first order plant Y_p, the crossover frequency can be calculated as $\omega_c = 4.88 rad/sec$. With ω_c in hand, we can choose an arbitrary α. For this simulation, the reference model is chosen as a unity feedback system with the open loop transfer function as $Y_{OL}(s) = \frac{4.88(s+1)}{s(s+1)} e^{-0.3s}$.

Figures 2 and 3 illustrates the adaptive parameters. It is seen that at $t = 25sec$, the adaptive parameters vary due to the effort to compensates the plant changes. Figure 4 shows the forcing function and the human command to the plant which tries to follow the forcing function. Also, figure 5 shows the error between human-plant system states and

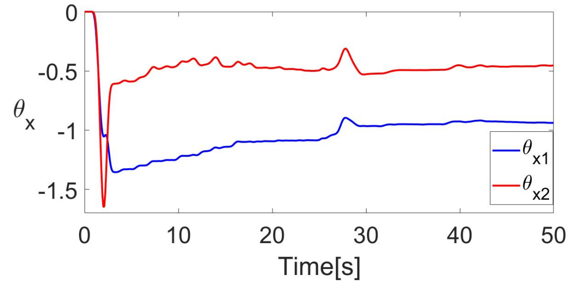

Fig. 2: Adaptive parameters.

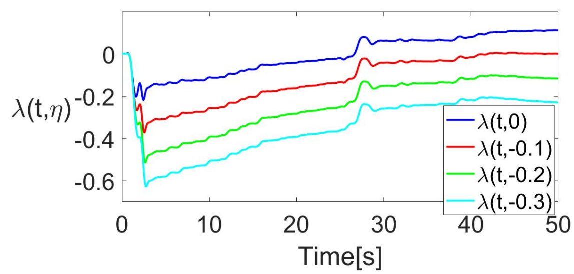

Fig. 3: Adaptive parameters for different η values.

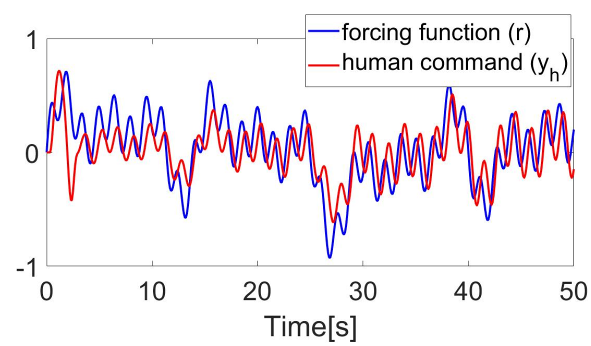

Fig. 4: Human (red line) is trying to follow the forcing function (blue line).

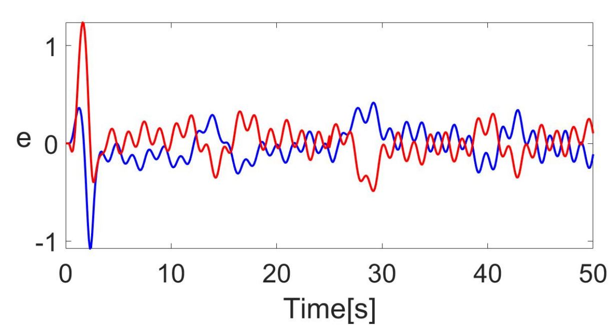

Fig. 5: Tracking error $e = x_{hp} - e_m$.

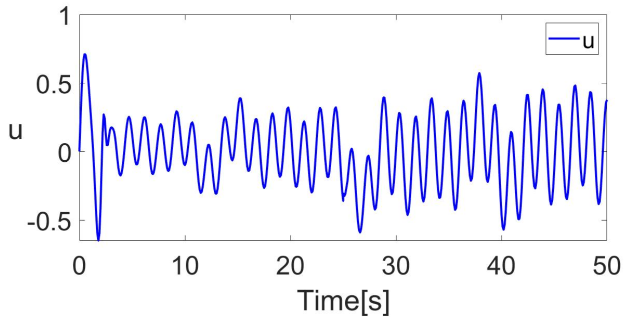

Fig. 6: Human adaptive decision-making signal.

reference model states. It is seen that the error in the first three seconds are large which is due to the bad parameters' estimation in the first three seconds. In figure 6, the human decision-making signal is shown. It is seen that the human decision changes at $t = 25sec$ in order to compensate the changes in plant.

VI. CONCLUSIONS

In this paper, a new human model based on the adaptive model reference control was proposed. This model mimics the human decision making process which follows the crossover model while the plant is uncertain. This time-varying human model can be used for human-in-the-loop stability analysis since the adaptive laws are obtained using the Lyapunov-Krasovskii stability criteria. In addition, it does not require any system identification method neither for the human model parameters nor for the plant uncertainties. The simulations performed using the proposed human model show the time-varying human model gains and successful reference tracking.

REFERENCES

[1] W. D. Nothwang, R. M. Robinson, S. A. Burdenand, M. J. McCourt, and J. W. Curtis, "The human should be part of the control loop?," *Resilience Week (RWS)*, 2016.

[2] M. Körber, W. Schneider, and M. Zimmermann, "Vigilance, boredom proneness and detection time of a malfunction in partially automated driving," *International Conference on Collaboration Technologies and Systems (CTS)*, 2015.

[3] D. M. Acosta, Y. Yildiz, R. W. Craun, S. D. Beard, M. W. Leonard, G. H. Hardy, and M. Weinstein, "Piloted evaluation of a control allocation technique to recover from pilot-induced oscillations," *J. Aircraft*, vol. 52, pp. 130-140, 2015.

[4] Y. Yildiz, and I. V. Kolmanovsky, "A control allocation technique to recover from pilot-induced oscillations (CAPIO) due to actuator rate limiting," *American Control Conference (ACC)*, pp. 516-523, 2010.

[5] Y. Yildiz, I. V. Kolmanovsky, and D. Acosta, "A control allocation system for automatic detection and compensation of phase shift due to actuator rate limiting," *American Control Conference (ACC)*, pp. 444-449, 2011.

[6] S. S. Tohidi, Y. Yildiz, and I. Kolmanovsky, "Pilot induced oscillation mitigation for unmanned aircraft systems: an adaptive control allocation approach," *IEEE Conference on Control Technology and Applications (CCTA)*, Copenhagen, Denmark, Aug. 2018.

[7] W. Li, D. Sadigh, S. S. Sastry, and S. A. Seshia, "Synthesis for human-in-the-loop control systems," *TACAS Conference*, 2014.

[8] T. Yucelen, Y. Yildiz, R. Sipahi, E. Yousefi, and N. Nguyen, "Stability limit of human-in-the-loop model reference adaptive control architecture," *International Journal of Control*, vol. 91, pp. 2314-2331, 2018.

[9] M. Xia, A. Rahnama, S. Wang, and P. J. Antsaklis, "On guaranteeing passivity and performance with a human controller," *Mediterranean Conference on Control and Automation*, Torremolinos, Spain, Jul. 2015.

[10] R. Sipahi, and, S. -I. Niculescu, "Stability of car following with human memory effects and automatic headway compensation," *Phil. Trans. R. Soc.*, vol. 368, pp. 4563-4583, 2010.

[11] T. P. Neal, and R. E. Smith, "An in-flight investigation to develop control system design criteria for fighter airplanes," Wright-Patterson Air Force Base, Ohio, USA: Air Force Flight Dynamics Laboratory, 1970.

[12] D. T. McRuer, and E. S. Krendel, "Human pilot dynamics in compensatory systems," Wright-Patterson Air Force Base, Ohio, USA: Air Force Flight Dynamics Laboratory, 1965.

[13] G. C. Beerens, H. J. Damveld, M. Mudler, and M. M. van Paassen, "An investigation into crossover regression and pilot parameter adjustment *AIAA Modeling and Simulation Technologies Conference and Exhibit*, 2008.

[14] D. T. Mcruer, and H. Jex, "A review of quasi-linear pilot models," *IEEE Transactions on human Factors in Electronics*, vol. 8, pp. 231-249, 1967.

[15] P. M. T. Zaal, and B. T. Sweet, "Estimation of time-varying pilot model parameters," *AIAA Modeling and Simulation Technologies Conference*, Portland, OR, USA, Aug. 2011.

[16] R. F. M. Duarte, D. M. Pool, and M. M. van Paassen, "Experimental scheduling functions for global LPV Human controller modeling," *IFAC*, Jul. 2017.

[17] X. Zhang,T. M . Seigler, and J. B. Hoagg, "Modeling the control strategies that humans use to control nonminimum-phase systems," *American Control Conference*, Chicago, IL, USA, Jul. 2015.

[18] R. A. Hess, "Modeling pilot control behavior with sudden changes in vehicle dynamics," *Journal of Aircraft*, vol. 46, pp. 1584-1592, 2009.

[19] R. A. Hess, "Modeling human pilot adaptation to flight control anomalies and changing task demands," *Journal of Guidance, Control and dynamics*, vol. 39, pp. 655-666, 2016.

[20] M. Lone, and A. Cooke, "Review of pilot models used in aircraft flight dynamics," *Aerospace Science and Technology*, vol. 34, pp. 55-74, 2014.

[21] S. Xu, W. Tan, A. V. Efremov, L. Sun, and X. Qu, "Review of control models for human pilot behavior," *Annual Reviews in Control*, vol. 44, pp. 274-291, 2017.

[22] R. E. Magdaleno, and X. Qu, "Experimental validation and analytical elaboration for models of the pilot's neuromuscular subsystem in tracking tasks," *Systems Technology, Inc.*, Hawthorne, California, 1971.

[23] Y. Yildiz, A. Annaswamy, I. Kolmanovsky, and D. Yanakiev, "Adaptive posicast controller for time-delay systems with relative degree $n^* \geq 2$," *Automatica*, vol. 46, pp. 279-289, 2010.

[24] S. -I. Niculescu, and A. Annaswamy, "An adaptive smith-controller for time delay systems with relative degree $n^* \leq 2$," *Systems and Control Letters*, vol. 49, pp. 347-358, 2003.

[25] X. M. Yang, X. Q. Yang,and K. L. Teo, "A matrix trace inequality," *Journal of Mathematical Analysis and Applications*, vol. 263, no. 1, pp. 327-331, 2001.

[26] H. G. H. Zollner, D. M. Pool, H. J. Damveld, M. M. van Paassen, and M. Mulder, "The effects of controlled element break frequency on pilot dynamics during compensatory target-following," *AIAA Modeling and Simulation Technologies Conference*, Aug. 2010.